Extended Source Localization using the ESPRIT Algorithm

S. Shahbazpanahi[1], *S. Valaee*[2,1], *B. Champagne*[3], *P. Kabal*[4]

[1] Dept. of Elect. Eng., Sharif University of Technology, Tehran, Iran
[2]Dept. of Elect. Eng., Tarbiat Modares University, Tehran, Iran
[3]INRS-Telecommunications, Verdun, Quebec, Canada
[4]Dept. of Elect. Eng., McGill University, Montreal, Canada

ABSTRACT: *A new approach to parametric localization of a distributed source is proposed. This method is based on the ESPRIT Algorithm. the Central angle and the angular extension of an incoherently distributed source are estimated. This algorithm has a low computational complexity. The method does not require array calibration*

1 Introduction

Array signal processing is used to detect and localize signal emitting sources. Several algorithms ranging from the low to high resolution techniques have been proposed in the literature.

The conventional array processing techniques assume *point source* modeling. By a point source, we mean that the radiated energy is emitted from a discrete angle in space. Various algorithms have been developed for point source localization. Among these methods, MUSIC [1] and ESPRIT [2] [3] are well-known. MUSIC carries out a one-dimensional search over the MUSIC spatial spectrum to find its prominant peaks. The location of these peaks corresponds to the estimate of the Direction Of Arrivals (DOA). In constructing the MUSIC spectrum, one needs to measure the *array manifold*, the set of possible steering vectors over all angular parameters. This is called array *calibration* which is practically expensive. An alternative is to use the ESPRIT algorithm which does not need array calibration.

The point source modeling may fail in certain practical situations. For example, the variation of sound speed in water may cause energy be distributed over an angular volume in a bottom-mounted passive sonar. In an undersea echo beam sounder, scattered signal from lower layers is distributed over an angular volume which is equivalent to a superposition of planewaves originating from a continum of angles [4]. Other examples are acoustic sources in a reverberant room, tropospheric or ionospheric propagation of radio waves, the reflection of a low radio link signal from ground, etc. The above examples show the importance of the *distributed source* modeling.

Jantii [4] models a distributed source as a sum of finite number of point sources and then estimates the angle of arrival of those point sources using the MUSIC and ESPRIT algorithms. A shortcoming of this technique is that for unique localization of sources, the number of point sources must be upper bounded by the number of sensors [5]. Furthermore, inference of the spatial extension using the point source location estimate is not clear.

Valaee et.al. [6] have presented a parametric method for localization of distributed sources. They generalize the concept of the signal and noise subspaces and derive a MUSIC-type spatial spectrum estimator. Similar to the original MUSIC algorithm, their approach also requires array manifold calibration.

In this paper, a new technique is presented for estimation of the central angle and the angular extension of a *uniform incoherently distributed* (UID) source. Estimation of the central angle is performed using an ESPRIT-type algorithm. Hence, there is no need for array calibration. The angular extension is estimated using the eigenvalues of covariance matrix. It is shown that the covarinace matrix for a uniformly distributed source can be represented in terms of the Discrete Prolate Spheroidal Sequences (DPSS) [8].

The paper is organized as follows. In the next section, the array output model for distributed sources is presented. Properties for the uniform linear array (ULA) covariance matrix is expressed

in Section 3. Section 4 summerizes the estimation algorithm and Section 5 contains the simulation results.

2 Distributed Source Modeling

Consider an array of $2p$ sensors (p doublets). Assume that the two sensors in each doublet are identical and have the same gain and phase and sensitivity pattern and are seperated by a constant displacement vector d. It means that the array is divided into two subarrays. We call them the X and Y subarrays. Also, it is assumed that q narrowband distributed sources with central frequency ω_0 are present in the environment of these subarrays. The complex envelope of the output of ith sensor in subarray X is

$$x_i = \sum_{m=1}^{q} \int_{-\frac{\pi}{2}}^{\frac{\pi}{2}} a_i(\theta) s(\theta, \psi_m) d\theta + n_{x_i} \qquad (1)$$

where $a_i(\theta)$ is the response of the ith sensor to a unit energy source emitting at direction θ, $s(\theta, \psi_m)$ is the angular density of the mth source, ψ_m is the mth source location parameter vector, and n_{x_i} is the additive zero mean noise at the ith sensor. The corresponding element output in subarray Y is

$$y_i = \sum_{m=1}^{q} \int_{-\frac{\pi}{2}}^{\frac{\pi}{2}} a_i(\theta) e^{-j\omega_0 \tau(\theta)} s(\theta, \psi_m) d\theta + n_{y_i} \quad (2)$$

where n_{y_i} is the additive zero mean noise at the ith sensor of the subarray Y, and $\tau(\theta)$ is the propagation delay between the identical elements of a doublet for the signal arriving at the direction θ. Using a vector notation, we have

$$\mathbf{x} = \sum_{m=1}^{q} \int_{-\frac{\pi}{2}}^{\frac{\pi}{2}} \mathbf{a}(\theta) s(\theta, \psi_m) d\theta + \mathbf{n}_x, \qquad (3)$$

$$\mathbf{y} = \sum_{m=1}^{q} \int_{-\frac{\pi}{2}}^{\frac{\pi}{2}} e^{-j\omega_0 \tau(\theta)} \mathbf{a}(\theta) s(\theta, \psi_m) d\theta + \mathbf{n}_y \quad (4)$$

where $\mathbf{x}$ and $\mathbf{y}$ are the subarray X and Y output vectors, respectively, $\mathbf{n}_x$ and $\mathbf{n}_y$ are the noise vectors for subarray X and Y, $\mathbf{a}(\theta)$ is the location vector for a source at the direction θ.

For uncorrelated sources, the covariance matrix at the output of array X and the cross-covariance matrix between the two subarrays are [6]

$$\mathbf{R}_{xx} = \sum_{m=1}^{q} \int_{-\frac{\pi}{2}}^{\frac{\pi}{2}} \int_{-\frac{\pi}{2}}^{\frac{\pi}{2}} \mathbf{a}(\theta) \rho(\theta, \theta'; \psi_m) \mathbf{a}^H(\theta') d\theta d\theta' + \sigma_n^2 \mathbf{I}, \quad (5)$$

$$\mathbf{R}_{xy} = \sum_{m=1}^{q} \int_{-\frac{\pi}{2}}^{\frac{\pi}{2}} \int_{-\frac{\pi}{2}}^{\frac{\pi}{2}} \mathbf{a}(\theta) \rho(\theta, \theta'; \psi_m) e^{j\omega_0 \tau(\theta')} \mathbf{a}^H(\theta') d\theta d\theta' \quad (6)$$

where σ_n^2 is the noise power and

$$\rho(\theta, \theta'; \psi_m) \triangleq \mathrm{E}\{s(\theta, \psi_m) s(\theta', \psi_m)\} \qquad (7)$$

is the *angular cross correlation* for the source m.

If different rays of the signal which arrive at the array are uncorrelated, the source is called an *incoherently distributed* (ID) source. This model has been introduced in [9] and [6]. For an ID source, we have

$$\mathrm{E}\{s(\theta, \psi_m) s^*(\theta', \psi_m)\} = \rho(\theta, \psi_m) \delta(\theta - \theta') \quad (8)$$

where $p(\theta, \psi_m)$ is called the *angular power density*.

3 ULA Covariance Matrix

For a uniform linear array with interelement spacing $\frac{\lambda}{2}$ (half the signal wavelength), the response of the ith sensor for a signal arriving at the angle θ made with the array broadside is

$$a_i(\theta) = e^{j(i-1)\pi \sin(\theta)}. \qquad (9)$$

Therefore, for a single ID source scenario, the mnth element of the covariance matrix can be written as

$$[\mathbf{R}_{xx}]_{mn} = \int_{-\frac{\pi}{2}}^{\frac{\pi}{2}} e^{j(m-n)\pi \sin\theta} \rho(\theta, \psi) d\theta + \sigma_n^2 \delta_{m-n}. \qquad (10)$$

For a uniformly distributed source,

$$\rho(\theta, \psi) = \begin{cases} \frac{1}{2\Delta} & \text{if } |\theta - \theta_0| < \Delta \\ 0 & \text{otherwise} \end{cases} \qquad (11)$$

where θ_0 is the source central angle and Δ is the source half extension width,

$$[\mathbf{R}]_{xx} = \int_{\theta_0 - \Delta}^{\theta_0 + \Delta} \frac{1}{2\Delta} e^{j(m-n)\pi \sin(\theta)} d\theta + \sigma_n^2 \delta_{m-n}. \qquad (12)$$

For small Δ, it can be shown that [4], [7]

$$[\mathbf{R}_{xx}]_{mn} = e^{j(m-n)\pi \sin(\theta_0)} \times \frac{\sin\Big((m-n)\pi\Delta\cos(\theta_0)\Big)}{(m-n)\pi\Delta\cos(\theta_0)} + \sigma_n^2 \delta_{m-n} \quad (13)$$

Define

$$W \triangleq \frac{\Delta}{2}\cos(\theta_0), \tag{14}$$

and the $p \times p$ matrix $\mathbf{M}(W)$ as

$$[\mathbf{M}(W)]_{mn} \triangleq \frac{\sin(2\pi W(m-n))}{\pi(m-n)}. \tag{15}$$

Then

$$[\mathbf{R}_{xx}]_{mn} = \frac{1}{2W}e^{j(m-n)\pi\sin(\theta_0)}[\mathbf{M}(W)]_{mn} + \sigma_n^2\delta_{m-n} \tag{16}$$

which can also been written as

$$\mathbf{R}_{xx} = \frac{1}{2W}\mathbf{D}\mathbf{M}(W)\mathbf{D}^H + \sigma_n^2\mathbf{I} \tag{17}$$

where

$$\mathbf{D} = \mathrm{diag}(1, e^{j\pi\sin\theta_0}, \ldots, e^{j\pi(p-1)\sin\theta_0}). \tag{18}$$

diag(·) is a representation for a diagonal matrix with the diagonal elements in the parantheses. The eigenvectors of $\mathbf{M}(W)$ are the Discrete Prolate Spheroidal Sequences (DPSS)[8]. A good approximation to the eigenvalues of $\mathbf{M}(W)$ is [8]

$$\lambda_k(W) \approx \frac{1}{\pi}(2\pi W)^{2k+1}G(k,p) \quad k = 0, 1, \ldots, p-1 \tag{19}$$

where

$$G(k,p) = \frac{2^{2k}(k!)^6}{(2k+1)^2(2k!)^4}\prod_{j=-k}^{k}(p-j). \tag{20}$$

It can be seen that

$$\lambda_0 \approx 2Wp, \tag{21}$$

$$\lambda_1 \approx \frac{1}{36}(p-1)p(p+1)\pi^2(2W)^3. \tag{22}$$

In the same manner, it can be shown that for the array configuration shown in Fig.1(a), the cross covariance matrix, is

$$\mathbf{R}_{xy}^{(a)} = \frac{e^{j2\pi d/\lambda\sin(\theta_0)}}{2W}\mathbf{D}\mathbf{M}'(W)\mathbf{D}^H \tag{23}$$

where

$$[\mathbf{M}'(W)]_{mn} = \frac{\sin\Big(2\pi W(m-n-2d/\lambda)\Big)}{\pi(m-n-2d/\lambda)}. \tag{24}$$

The superscript (a) represents the correlation matrix associated with Fig.1(a). For the array configuration shown in Fig.1(b), it is easy to show that

$$\mathbf{R}_{xy}^{(b)} = \frac{e^{j2\pi d/\lambda\sin(\theta_0)}}{2W}\mathbf{D}\mathbf{M}''(W)\mathbf{D}^H \tag{25}$$

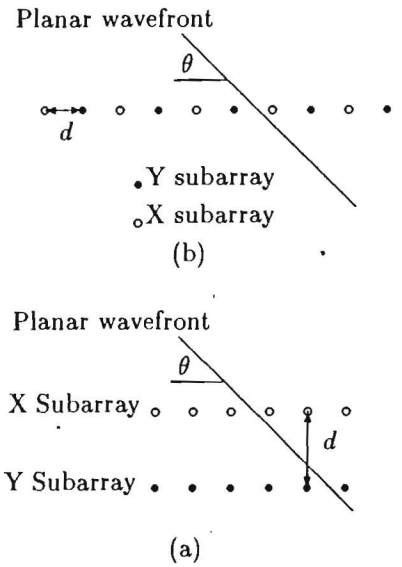

Figure 1: Two possible subarray configurations.

where

$$[\mathbf{M}''(W)]_{mn} = \frac{\sin\Big(2\pi W(m-n-2d/\lambda\tan\theta_0)\Big)}{\pi(m-n-2d/\lambda\tan(\theta_0))}. \tag{26}$$

In the above equations, d is the magnitude of displacement vector between the two subarrays.

4 Estimation Algorithm

The proposed estimation technique is summarized as follows:

1. The central angle is estimated using the TLS-ESPRIT algorithm [2]. TLS-ESPRIT is implemented in four steps:

   (a) Let

   $$\mathbf{z} = \begin{bmatrix} \mathbf{x} \\ \mathbf{y} \end{bmatrix}, \tag{27}$$

   and define $\mathbf{R}_{zz}$ as

   $$\mathbf{R}_{zz} \triangleq \mathrm{E}\{\mathbf{z}\mathbf{z}^H\} = \begin{bmatrix} \mathbf{R}_{xx} & \mathbf{R}_{xy} \\ \mathbf{R}_{yx} & \mathbf{R}_{xx} \end{bmatrix}, \tag{28}$$

   and let $\mathbf{e}_0$ be the eigenvector of $\mathbf{R}_{zz}$ corresponding to the largest eigenvalue of $\mathbf{R}_{zz}$.

   (b) Then $\mathbf{e}_0$ is written as

   $$\mathbf{e}_0 = \begin{bmatrix} \mathbf{e}_{0X} \\ \mathbf{e}_{0Y} \end{bmatrix}, \tag{29}$$

   where $\mathbf{e}_{0X}$ and $\mathbf{e}_{0Y}$ are the upper and the lower half of $\mathbf{e}$, respectively.

(c) Define $\mathbf{E}_{XY}$ as

$$\mathbf{E}_{XY} \stackrel{\Delta}{=} [\mathbf{e}_{0X} \quad \mathbf{e}_{0Y}]. \tag{30}$$

Compute the eigendecomposition of $\mathbf{E}_{XY}^H \mathbf{E}_{XY}$,

$$\mathbf{E}_{XY}^H \mathbf{E}_{XY} = \mathbf{E}\mathbf{\Lambda}\mathbf{E}^H. \tag{31}$$

For a single distributed source, $\mathbf{E}$ is a 2×2 matrix and can be written as

$$\mathbf{E} = \begin{bmatrix} E_{11} & E_{12} \\ E_{21} & E_{22} \end{bmatrix} \tag{32}$$

(d) For Fig.1(a), θ_0 is estimated as

$$\hat{\theta}_0 = \sin^{-1}\{\frac{\lambda \arg(-E_{12}/E_{22})}{2\pi d}\} \tag{33}$$

and for Fig.1(b), θ_0 is estimated as

$$\hat{\theta}_0 = \cos^{-1}\{\frac{\lambda \arg(-E_{12}/E_{22})}{2\pi d}\} \tag{34}$$

2. According to Equation (13) it is clear that

$$[\mathbf{R}_{xx}]_{mm} = 1 + \sigma_n^2. \tag{35}$$

Hence the noise power estimate, $\hat{\sigma}_n^2$ is

$$\hat{\sigma}_n^2 = \min\{\mathrm{diag}(\mathbf{R}_{xx})\} - 1. \tag{36}$$

The noise free covariance matrix

$$(\mathbf{R}_{xx})_{NF} = \frac{1}{2W}\mathbf{D}\mathbf{M}(W)\mathbf{D}^H \tag{37}$$

can be estimated from

$$(\mathbf{R}_{xx})_{NF} = \mathbf{R}_{xx} - \hat{\sigma}_n^2\mathbf{I} \tag{38}$$

3. The parameter W is estimated using (22). Let l_1 be the second eigenvalue of $(\mathbf{R}_{xx})_{NF}$. From (22) and (37), we have

$$l_1 = \frac{\lambda_1}{2W} = \frac{1}{36}(p-1)p(p+1)4\pi^2W^2. \tag{39}$$

Hence

$$W = \frac{3}{\pi}\sqrt{\frac{l_1}{(p-1)p(p+1)}}. \tag{40}$$

Note that the first eigenvalue of $(\mathbf{R}_{xx})_{NF}$ can not be used for the estimation of W. In fact, from (21) and (37) it is clear that the largest eigenvalue of $(\mathbf{R}_{xx})_{NF}$ is approximately independent from W, that is

$$l_0 \approx p \tag{41}$$

4. Having W and θ_0, one can estimate Δ using

$$\Delta = 2W/\cos\theta_0. \tag{42}$$

5 Simulation

In this section, the computer simulations are presented. The simulated array consists of 32 omnidirectional sensors, 16 sensors in each subarray. The two subarrays are displaced from each other as shown in Fig. 1(a) with $d = \lambda/15$. the source power is distributed uniformly and incoherently over the angular interval $[\theta_0 - \Delta, \theta_0 + \Delta]$, where $\theta_0 = 30\,\mathrm{deg}$. Parameter Δ is chosen to be $1, 2, 3$ and 4 degrees in different trials.

Fig. 2 and Fig. 3 show the bias and the variance of the central angle estimation, respectively, for different values of Δ.

Fig. 4 and Fig. 5 show the bias and the variance of the extension width estimate, Δ, respectively, for different values of Δ.

References

[1] R. O. Schmidt, "Multiple emitter location and signal parameter estimation," *IEEE Trans. Antenn. Propagat.*, vol. AP-34, pp. 276-280, Mar. 1986.

[2] R. Roy and T. Kailath, "ESPRIT-Estimation of Signal Parameters via Rotational Invariance Techniques," *IEEE Trans. Acoust., Speech, Signal Processing*, vol. 37, no.7, pp. 984-995, July 1989.

[3] R. Roy, A. Paulraj and T. Kailath, "Direction of arrival estimation by subspace rotation methods-ESPRIT," in *Proc. IEEE Int. Conf. Acoust., Speech, Signal Processing,* Tokyo, 1986, pp. 47.2.1-47.2.4.

[4] T. P. Jantii, "The influence of extended sources on the theoretical performance of the MUSIC and ESPRIT methods: Narrow band sources," in *Proc. IEEE Int. Conf. Acoust., Speech, Signal Processing,* San Francisco, Mar 1992, pp. II-429-II432.

[5] M. Wax, "On unique localization of constrained-signal sources," *IEEE Trans. Signal Processing,* vol. 40, pp.1542-1547, June 1992.

[6] S. Valaee, B. Champagne and P. Kabal, "Parametric localization of distributed sources," *IEEE Trans. Signal Processing,* vol. 43, no. 9, pp.2144-2153, Sep. 1995.

[7] S. Shabazpanahi, S. Valaee and M. M. Nayebi, "Spatial parameters estimation

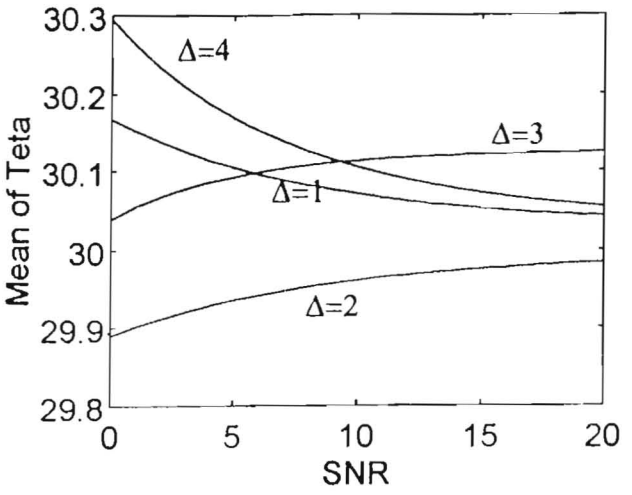

Figure 2: The mean of the estimate of the central angle θ_0 for different values of the extension width Δ.

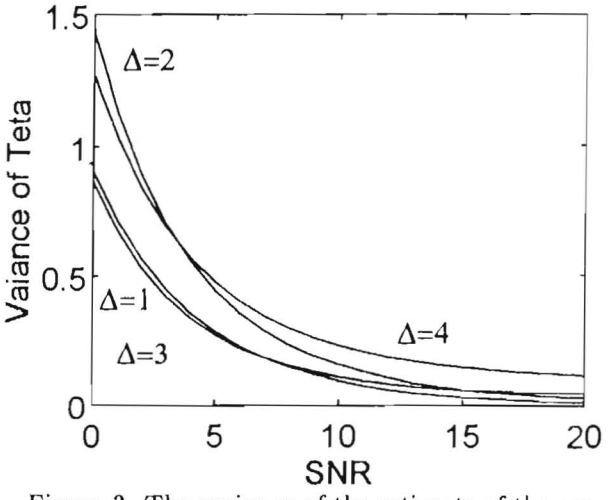

Figure 3: The variance of the estimate of the central angle θ_0 for different values of the extension width Δ.

of distributed source," *submitted to Iranian Conf. Electrical Engineering (ICEE97)*, Tehran, Iran.

[8] D. Slepian, "Prolate spheroidal wave functions, fourier analysis, and uncertainty-V: the discrete case," *The Bell System Technical Journal*, pp. 1371-1430. May-June 1978.

[9] S. Haykin Ed. *Array Signal Processing*. Englewood Cliffs, NJ:Prentice-Hall, 1985.

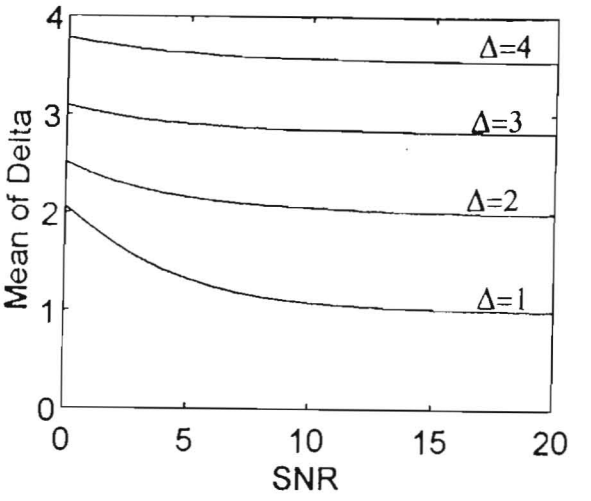

Figure 4: The mean of the estimate of the extension width Δ.

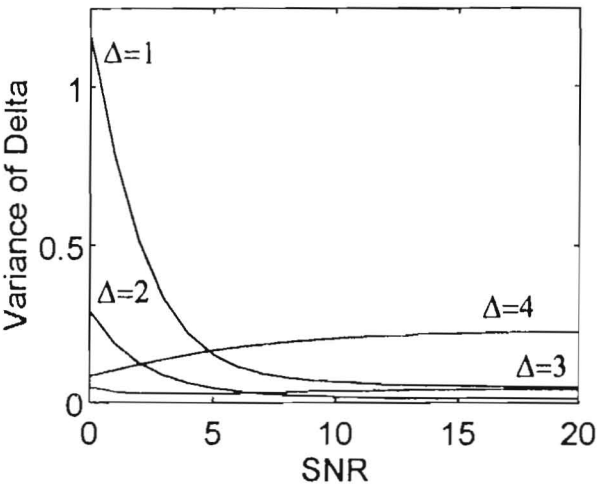

Figure 5: The variance of the estimate of the extension width Δ.